Adv. Theor. Appl. Mech., Vol. 1, 2008, no. 7, 301 - 314

Nonlinear Vibration Signature Analysis of High Speed Rotor Due to Defects of Rolling Element

S. H. Upadhyay[*], S. P. Harsha and S. C. Jain

Mechanical & Industrial Engineering Department
Indian Institute of Technology Roorkee, India
upadhyaysanjayh@yahoo.com, surajfme@iitr.ernet.in
sjainfme@iitr.ernet.in

Abstract

This paper presents a mathematical model to investigate the nonlinear dynamic behavior of a high speed rotor-bearing system due to defects of rolling elements. ***Two defects*** have been considered for the study, one defect as off-sized rolling elements and other defect as rolling element waviness. In the formulation, the contacts between rolling elements and inner/outer races are considered as nonlinear springs and also used nonlinear damping, which is developed by correlating the contact damping force with the equivalent contact stiffness and contact deformation rate. The equations of motion are formulated using Lagrange's equation, considering the vibration characteristics of the individual components such as inner race, outer race, rolling elements and rotor. The highest radial vibrations due to ball size variation are at a speed of the number of balls times the cage speed ($\omega_{bp} = N_b\, \omega_{cage} Hz$). The other vibrations due to ball size variation are also occur at $\omega_{bp} \pm k\omega_{cage}$, where k is a constant. Due to ball waviness, nonlinear dynamic responses are found to be associated mainly with wave passage frequency (ω_{wp}) and ball passage frequency (ω_{bp}) with their interactive effects.

Keywords: Nonlinear dynamics, rolling bearing, ball passage frequency, wave passage frequency, Poincaré maps

[*] **Corresponding Author** [*] sanjudme@iitr.ernet.in

Nomenclature

k_{in}	equivalent non-linear contact stiffness of the roller-inner race contact
k_{out}	equivalent non-linear contact stiffness of the roller-outer race contact
$k_{in\text{-}contact}$	contact stiffness of the roller-inner race contact
$k_{out\text{-}contact}$	contact stiffness of the roller-outer race contact
m_{rotor}	mass of the rotor, kg
N_b	number of balls
Δd_p	change in diameter of rolling element
δ_{in}	contact deformation of the roller-inner race
δ_{out}	contact deformation of the roller-outer race
$\delta\theta$	angular displacement due to off-sized rolling element
ω_{cage}	angular velocity of cage, rad/s
ω_{inner}	angular velocity of the inner race, rad/s
ω_{outer}	angular velocity of the outer race, rad/s
ω_{bp}	ball passage frequency, Hz
ω_{wp}	wave passage frequency, Hz
$(\Pi)_{in}$	amplitude of the wave at inner race
$(\Pi)_{out}$	amplitude of the wave at outer race
FFT	fast Fourier transformation
BPF	ball passage frequency, Hz
BPV	ball passage vibration, Hz
WPF	Wave Passage Frequency, Hz

1 Introduction

An analysis of rolling bearing dynamic response is important to predict the system behavior. The rotor bearing assembly, which is supported by perfect rolling bearings, the vibration spectrum is dominated by the vibrations at the natural frequency and the ball passage frequency (BPF). The vibrations at this later frequency are called ball passage vibrations (BPV). The other vibrations are generated by geometrical imperfections of the individual bearing components and these imperfections are caused by irregularities during the manufacturing process. The imperfection such as surface waviness in the races developed during manufacturing process; produce significant vibrations in the system.

Ball passage vibrations were first documented, by Perret [1] and Meldau [2] as a static running accuracy problem. Gad et al. [3] showed that resonance occurs when BPF coincides with frequency of the system and they also pointed out that for certain speeds, BPF can exhibit its sub and super harmonic vibrations for rotor ball bearing system. Rahnejat and Gohar [4] showed that even in the presence of elasto-hydrodynamic lubricating film between balls and the races, a peak at the BPF appears in the spectrum. They suggested that the limit cycle frequency and amplitude is affected by the number of balls, applied load and radial internal clearance. Wardle [5] theoretically and experimentally showed that ball waviness

produced vibrations in the axial and radial directions at different frequencies and also pointed out that only even orders of ball waviness produced vibrations. They also showed that the outer race waviness produces vibrations at the harmonics at outer race ball passage frequency.

Aktürk et al [6] performed a theoretical investigation of effect of varying the preload on the vibration characteristics of a rotor bearing system and also suggested that by taking correct number of balls and amount of preload in a bearing untoward effect of the BPV can be reduced. Aktürk [7] presented the effect of surface waviness on vibrations associated with ball bearings and conclude that for outer race waviness most sever vibrations occur when the BPF and its harmonics coincide with the natural frequency.

Harsha et al. [8] developed an analytical model to predict nonlinear dynamic response in a rotor bearing system due to surface waviness. The conclusion of this work shows that for the outer race waviness, the severe vibrations occur when the number of balls and waves are equal. In case of the inner race waviness, the peak amplitude of vibration can be at $q\omega_{wp} \pm p\omega_{cage}$. For the waviness order iN_b, peak amplitude of vibration and super-harmonic appear at the wave passage speed (ω_{wp}). Harsha et al [9] have studied the stability analysis of a rotor bearing system due to surface waviness and number of balls. They suggested that the system express dynamic behaviors that are extremely sensitive to small variations of the system parameters, such as number of balls and number of waves. Harsha et al [10] have been studied the effects of ball waviness associate with rolling element bearing. The appearance of periodic, sub-harmonic, chaotic and Hopf bifurcation is seen theoretically. But he has considered only nonlinear stiffness.

In this paper, a theoretical investigation is conducted to observe the effects of off size rolling elements and rolling element waviness with varying the number of balls on the vibration characteristics of a rotor bearing system. A nonlinear damping formula, correlating the contact damping force with the equivalent contact stiffness and contact deformation rate (determined by the surface profiles and radial speed of inner/outer races and rollers), is developed to improve model fidelity.

2 Problem Formulations

A schematic diagram of rolling element bearing is shown in Fig.1 (a). For investigating the structural vibration characteristics of rolling element bearing, a model of bearing assembly can be considered as a spring mass damper system. Elastic deformation between races and rollers gives a non-linear force deformation relation, which is obtained by Hertzian theory. In the mathematical modeling, the rolling element bearing is considered as spring mass system and rolling elements act as non-linear contact spring as shown in Fig. 1(b). Since, the Hertzian forces arise only when there is contact deformation, the springs are required to act only in compression. In other words, the respective spring force comes into play when the instantaneous spring length is shorter than its unstressed length, otherwise the separation between balls and the races takes place and the

resultant force is set to zero. The excitation is because of the varying compliance vibrations of the bearing which arise because of the geometric and elastic characteristics of the bearing assembly varying according to the cage position
The rolling element bearing model considered here has equi-spaced balls rolling on the surfaces of the inner and outer races. For developing the theoretical model it is assumed that the outer race is fixed rigidly to the support and the inner race is fixed rigidly to the rotor and there is no bending of races.

$$\omega_{cage} = \omega_{rotor}\left(\frac{r}{r+R}\right) \quad \& \quad \omega_{bp} = \omega_{cage} \times N_b \tag{1}$$

Where, ω_{bp} is the ball passage frequency and N_b is the number of balls.

2.1 Rolling Element Waviness

An important source of vibrations in ball bearings is waviness. These are global sinusoidal shaped imperfections on the outer surface of the bearing components as shown in Fig. 2 (a). Waves are described in terms of two parameters: the wavelength (λ), which is the distance taken by a single cycle of the wave and its amplitude (Π) as shown in Fig. 2 (b). The characteristic wavelengths of the imperfections are much larger than the dimensions of the Hertzian contact areas between the balls and the guiding races. The number of waves per circumference is denoted by the wave number. Waviness imperfections cause variations in the contact loads when the bearing is running. The magnitude of the variation depends on the amplitude of the imperfection and the nonlinear stiffness and damping in the contact. Imperfections with a different wave number cause vibrations at distinct frequencies, each with a characteristic vibration mode.

Balls are free to spin about any axis and the axis may even change during the rotation. In order to calculate the waviness of balls, a simple case is considered where a ball with a perfectly sinusoidal wavy surface rotates about an axis as shown in Fig. 2 (a, b). The rolling element waviness causes a change in its diameter through contact with inner and outer races as

$$\Delta d_p = 2a_p \sin\left(N_w \theta_i\right) \tag{2}$$

Since, it is assumed that wave is sinusoidal; hence the amplitude of the rolling element waviness is,

$$\left(\Pi_i\right)_{r.e.} = 2a_p \sin\left(N_w \omega_{r.e.} t\right) \tag{3}$$

2.2 Ball diameter variations

When there are off-sized rolling elements in a rotor bearing system, this will cause an additional deflection differences. These differences can be larger or smaller than the rest, depending on the off sized rolling element diameter. Fig. 2 (c) shows that one ball has a greater diameter than the rest of balls in the set. Hence, for this off-sized rolling element, the equation of displacement of the j^{th} rolling element becomes (assuming the inner and outer races are rigid)

$$\delta\theta = \delta\theta_i + \Delta\Gamma \tag{4}$$

Where, $\Delta\Gamma$ is the diameter difference of the off-sized ball.

2.3 Formulation of Equations of Motion

A real rotor-bearing system is generally very complicated and difficult to model. First the expression for energies of the individual components of the bearing is formulated. Using these energies, the equations of motion are derived with the help of Lagrange's equation.

2.3.1 Energy Expressions

The total energy of system is considered to be the sum of kinetic energy, potential energy, strain energy of the springs representing contact and dissipation energy due to contact damping. The detail description of the energy expressions due to different parts of rolling bearings, which have already derived in the papers published by Harsha [10], are using in this paper. The contacts between rolling elements and races are treated as nonlinear springs, whose stiffness is obtained by Hertzian theory of elasticity. The nonlinear stiffness due to Hertzian contact effects and evaluated by equations, which is given in Appendix A. In those previous papers a constant damping value was chosen, but here a nonlinear viscous damping model is adopted.

2.3.2Energy Dissipation

The lubrication is assumed to behave in a Newtonian way. Hence, a viscous damping model is adopted in which the dissipative forces are proportional to the time derivate of the mutual approach. The resulting equation yields:

$$F_d = c(\delta)\dot{\delta}^{p} \tag{5}$$

Where $c(\delta)$ is also a function of the contact geometry, the material properties of the elastic bodies, the properties of the lubricant and the contact surface velocities, Hence, total energy dissipation can be calculated, which is given in Appendix B.

2.4 Equations of Motion

The kinetic energy and potential energy contributed by the inner race, outer race, balls, rotor and springs, can be differentiated with respect to the generalized coordinates ρ_j ($j = 1, 2, \ldots\ldots, N_b$), x_{in}, and y_{in} to obtain the equations of motion. For the generalized coordinate's $\boldsymbol{\rho_j}$, where $j = 1, 2 \ldots N_b$, the equations are:

$$\begin{aligned}
&\ddot{\rho}_j + g\sin\theta_j + \rho_j\dot{\theta}^2 - \frac{1}{m_j}\left(k_{in_contact}\right)\left[\delta_{in}\right]_+^{3/2}\frac{\partial\chi_j}{\partial\rho_j} + \frac{1}{m_j}\left(k_{out_contact}\right)\left[\delta_{out}\right]_+^{3/2} + \frac{1}{2m_j}\frac{\partial\left[\left(k_{in_contact}\right)\left[\delta_{in}\right]_+^{1/2}\right]}{\partial\rho_j}\left[\delta_{in}\right]_+^2 \\
&+ \frac{1}{2m_j}\frac{\partial\left[\left(k_{out_contact}\right)\left[\delta_{out}\right]_+^{1/2}\right]}{\partial\rho_j}\left[\delta_{out}\right]_+^2 + \frac{3}{2m_j}\sum_{j=1}^{N_{r.e}}\left\{C_{in}\left(k_{in_contact}\right)\delta_{in_+}^{3/2}\left(-\chi_j\right)^p\frac{\partial\chi_j}{\partial\dot{\rho}_j}\right\} \\
&+ \frac{3}{2m_j}\sum_{j=1}^{N_{r.e}}C_{out}\left(k_{out_contact}\right)\delta_{out_+}^{3/2}\left(-\dot{\rho}_j\right)^p = 0 \qquad j = 1,2,\ldots\ldots,N_{r.e}
\end{aligned} \tag{6}$$

For the generalized coordinate $\boldsymbol{x_{in}}$ the equation is:

$$\ddot{x}_{in} - \frac{1}{m_{rotation}}\sum_{j=1}^{N_{r.e}}\left(k_{in\_contact}\right)\left[\delta_{in}\right]_+^{3/2}\frac{\partial\chi_j}{\partial x_{in}} + \frac{3}{2m_{rotation}}\sum_{j=1}^{N_{r.e}}\left\{C_{in}\left(k_{in\_contact}\right)\delta_{in_+}^{3/2}\left(-\dot{\chi}_j\right)^p\frac{\partial\dot{\chi}_j}{\partial\dot{x}_{in}}\right\} = \frac{F_u\sin(\omega_s t)}{m_{rotation}} \tag{7}$$

For the generalized coordinate $\boldsymbol{y_{in}}$ the equation is:

$$\ddot{y}_{in}+g-\frac{1}{m_{rotation}}\sum_{j=1}^{N_{re}}\left(k_{in\_contact}\right)\left[\delta_{in}\right]_{+}^{3/2}\frac{\partial\chi_j}{\partial y_{in}}+\frac{3}{2m_{rotation}}\sum_{j=1}^{N_{re}}\left\{C_{in}\left(k_{in\_contact}\right)\delta_{in_{+}}^{3/2}\left(-\dot{\chi}_j\right)^{p}\frac{\dot{\chi}_j}{\dot{y}_{in}}\right\}=\frac{\left(W+F_u\cos(\omega_s t)\right)}{m_{rotation}} \qquad (8)$$

where $m_{rotation}=\left(m_{inner}+m_{rotor}\right)$

This is a system of (N_b + *2*) coupled non-linear differential equations. There is no external radial force is allowed to act on the bearing system and no external mass is attached to the outer race. The "+" sign as subscript in these equations signifies that if the expression inside the bracket is greater than zero, then the rolling element at angular location θ_j is loaded giving rise to restoring force and if the expression inside bracket is negative or zero, then the rolling element is not in the load zone, and restoring force is set to zero.

3. Methods of solution

The coupled non-linear second order differential equations are solved by numerical time integration technique. The non-analytic nature of the stiffness term renders the system equations difficult for analytical solution.

3.1. Numerical integration

The equations of motion (6)-(8) are solved using the modified Newmark-β method to obtain the radial displacement, velocity and acceleration of the rolling elements. With inclusion of damping, transient vibrations are eliminated and peak steady state amplitudes of vibration can be estimated. To observe the nonlinear behavior of the system, parameters of the ball bearing are selected and are shown in Table I. The time step for the investigation is taken as $\Delta t=10^{-5}$ *sec*.

4. Results and Discussion

The equations of motion are solved by modified Newmark-β method to obtain the radial displacement and velocity of the rolling elements. Two cases have been studied here one with off-sized rolling elements and other with rolling element waviness with varying the number of balls.

4.1 Effects of off-sized rolling elements

Owing to the different ball diameters, the race is deformed into a complex shape that turns with the rotational speed of the cage. The off-sized balls were located symmetrically in bearings such that they moved in the same direction simultaneously (i.e. the balls are assumed to be in phase). Firstly, two balls were assumed to be 0.2 μm oversized. The responses were obtained for the bearing with varying ball size of balanced rotor. The ball set rotated at the cage speed around the inner race and the oversized ball. Since, the ball set came to the same position after one cage rotation, the system underwent vibrations at a frequency

that was equal to the number of balls times the cage speed $N_b\omega_{cage}$.

When the number of balls (N_b) is 6, by way of Hopf bifurcation, the solution becomes unstable. The Poincaré map and orbit plot give an indication of a chaotic response as shown in Fig. 3 (a). Dense vibration spectrum shows a dominant peak at $\frac{1}{2}\omega_{bp} = 100\,Hz$. Other peaks are appeared at ω_{bp} = 200 Hz and $\omega_{bp} + 3\omega_{cage}$ = 300 Hz as shown in Fig.3 (a). As the wave-number and number of balls are increase to 7, the system shows quasi-periodic nature with weak attractor and the peak amplitude of vibration appears at $\frac{1}{2}\omega_{bp}$ = 116.66 Hz as shown in Fig. 3(b). Other peaks are appeared at ω_{bp} = 233.33 Hz and $\omega_{bp} + 3\omega_{cage}$ =333.32 as shown in the vibration spectrum.

This quasi-periodic nature of rotor bearing system and the peak of excitation in spectrum at $\frac{1}{2}\omega_{bp}$ Hz is remain till the number of balls is 9 as shown in Fig. 3 (c) (for $N_b = 8$) and Fig.3 (d) (for $N_b = 9$). Afterwards, a clear transformation is taking place in system nature as well as in the peak of excitation in the vibration spectrum as number of balls increases to 10 and above.

For the number of balls (N_b) is 13, by way of Hopf bifurcation, the solution becomes stable and shows periodic nature as shown in Fig. 3 (e). A clear peak of excitation is appearing in spectrum at $\omega_{bp} = 433.33\,Hz$. Similar trend is getting as the number of balls (N_b) is increased to 16, as shown in Fig. 3 (f).

Table II summarizes the relevant off size rolling elements, their peak amplitudes and harmonics in the bearing spectrum. The same trend for larger orders of off size balls can be expected.

4.2 Effects rolling element waviness

In order to study the effect of ball waviness, the ball is assumed to have wavy surface. The case is further simplified by assuming that the ball rotates about an axis passing through its center and parallel to the bearing axis. In the case of ball waviness, there are two important frequencies. The ball set rotates at the cage speed around the inner race and the ball with wavy surface acts like an oversized ball. Since the ball set came to the same position after one cage rotation, the system underwent vibrations at a frequency that was equal to the number of balls times the cage speed $N_b\omega_{cage}$. Other important frequency is ball rotation frequency (or, wave passage frequency) occurring at ball rotation speed $(\omega_{wp} = N_w\omega_{roll})$. When the ball rotates, the position of the balls will repeat itself after each $2/N_w$, where N_w is the number of waves per circumference of the rolling element. Therefore, the vibration due to rolling element waviness will take place at the speed of $N_w\omega_{roll}$.

Vibration response for ball waviness of order 6 (N_w=6) with 6 balls (N_b=6) is shown in Fig. 4 (a). A dominant peak appears in the vibration spectrum at ω_{wp} = 500 Hz and ω_{bp} = 200 Hz, with the other peaks appear at the interaction between both i.e. at $\omega_{wp} - \omega_{bp}/2$ = 400 Hz, and at $\omega_{wp} + \omega_{bp}/2$ = 600 Hz. The Poincaré

map in Fig. 4(a) gives an indication of a quasi-static response because of the 'net' structure.

With increase in wave order and ball as 7, the peak appears at ω_{bp} = 233.31 Hz in vibration response as shown in Fig. 4(b). Other peaks are at ω_{wp} = 583.31 Hz, and at $\omega_{wp} - \omega_{bp}$ = 350 Hz. Fig. 4(c) shows the vibration response for ball waviness of wave order 8. A dominant peak appears in the vibration spectrum at $\omega_{wp} - \omega_{bp}$ = 400 Hz, due to the interaction effect between wave passage and ball passage frequency. The other peaks are appeared at ω_{wp} = 666.64 Hz, ω_{bp} = 266.6 Hz. A similar trend of vibration spectrum and system responses is observing with increase number of ball and of same wave order, which has been summarized in Table – III.

5. Conclusions

A lumped parameter model has been introduced in this paper to investigate structural vibrations in roller bearings. Using this model, effect of ball waviness, off size number of balls, nonlinear stiffness and nonlinear damping on the vibration response of the bearing has been studied.

5.1 For off size Rolling Elements

The foregoing results provide the following conclusion:

- Nonlinear dynamic responses are found to be associated with ball passage frequency (ω_{bp}). Ball passage frequency is the system characteristics and the prediction about system behavior can be made by BPF to avoid resonance. When the number of balls is increased, the center of oscillations approaches zero implying a stiffer system. From this, it can be predicted that increasing the number of balls will reduce the effect of the BPF.
- From the observed response the effects of off size balls (N_b) on the system behavior can be analyzed and two different stages are obtained. For N_b =3 to N_b =9, the predicted peak appears at $\frac{1}{2}\omega_{bp}$ with other peaks of excitation appear at ω_{bp} and its interaction with ω_{cage} and also nature of solution is quasi-periodic. While for N_b =10 to N_b =19 the predicted peak appears at ω_{bp} and nature of solution is periodic.

When the number of balls is increased, the vibration reduces drastically implying a stiffer system; this was also reported by Aktürk et al. [6] from this it can be predicted that increasing the number of balls will reduce the effect of the modulating frequency and because of the ball passage frequency becomes dominant in the vibration spectrum.

5.2 For Rolling Element waviness

The foregoing results provide the following conclusion:

- It is observed from the vibration spectrum that the peak amplitude of vibrations due to ball waviness with varying number of balls appear at the wave passage frequency ($N_w\omega_{roll}$) and ball passage frequency ($N_b\omega_{cage}$). Increasing the number of waves means making the ball smoother with a larger diameter. When the $N_w\omega_{roll} \pm N_b\omega_{cage}$ coincides with the natural frequency of the system severe vibrations take place. Increasing the order of waviness will diminish the vibrations at the $N_w\omega_{roll} \pm N_b\omega_{cage}$ and only vibrations at the wave passage frequency will mainly remain in the spectrum. The axial vibrations are produced when the number of waves per circumference is an integral multiple of the ball rotation frequency in the bearing, which was proved experimentally by Wardle (1988b).

In this work, the effects of varying number of balls and wave-number of ball waviness are studied. Both are important parameters of study because, even if these are inevitable, these can be controlled the system nature to a good extent. From this analysis, a designer can choose the appropriate number of rolling elements with and without defects to avoid the severe vibrations (chaotic) condition.

Table I Geometric and Physical Properties used for the Ball Bearings

Ball radius	4.762 mm	Radial load (W)	6 N
Inner Race Diameter (D_i)	18.738 mm	Mass of rotor (m)	0.6 kg
Outer Race Diameter (D_o)	28.262 mm	Damping factor (c)	200 Ns/m
Internal radial clearance (γ)	10 μm	Pitch radius of the ball set (r_m)	27 mm
Ball radius	4.762 mm	Speed of the rotor (Nr)	5000 rpm

Table II Peaks for off size rolling elements

Number of Balls	**Peak Amplitude (μm)**	**Harmonic in Spectrum (μm)**
6	$\frac{1}{2}\ \omega_{bp}$	ω_{bp}, $\omega_{bp}+3\omega_{cage}$
7	$\frac{1}{2}\ \omega_{bp}$	ω_{bp}, $\omega_{bp}+3\omega_{cage}$
8	$\frac{1}{2}\ \omega_{bp}$	ω_{bp}, $\omega_{bp}+4\omega_{cage}$
9	$\frac{1}{2}\ \omega_{bp}$	ω_{bp}, $\omega_{bp}+4\omega_{cage}$
13	ω_{bp}	$2\omega_{bp}$
16	ω_{bp}	$2\omega_{bp}$

Table III Peaks for rolling element waviness

Number of Balls & Wave-number	**Peak Amplitude (μm)**	**Harmonic in Spectrum (μm)**
6	ω_{bp}, ω_{wp}	$\omega_{wp} \pm \frac{1}{2}\ \omega_{bp}$
7	ω_{bp}	ω_{wp}, ω_{wp} -ω_{bp}
8	ω_{wp} -ω_{bp}	ω_{wp}, ω_{bp}
9	ω_{bp}	ω_{wp}, ω_{wp} -ω_{bp}
13	ω_{bp}	ω_{wp}, ω_{wp} - ω_{bp}
16	$\frac{1}{2}\ \omega_{wp}$	ω_{wp}, ω_{bp}

References

[1] H. Perret. Elastic spielschwingungen konstant walzlger. Werkstalt und Betrieb ,3(1950),354–8.

[2] E .Meldau. Die bewegung der achse von walzlagern beigeringen drehzahlen. Werkstalt und Betrieb, 1955; 7–19.

[3] E.H.Gad, S. Fukata,H. Tamura. Computer simulation of rotor axial and radial vibrations due to ball bearings. Memories of the Faculty of Engineering, Kyushu University, 44 (1984), 169–189.
[4] H. Rahnejat, R Gohar. Vibration of radial ball bearing. Proceedings of the IMechE, 119(C3) (1985), 181-193.
[5] F.P. Wardle. Vibration forces produced by waviness of the rolling surfaces of thrust loaded ball bearings. Part I: Theory Proceedings of the IMechE, 202(C5) (1988), 305–312.
[6] N. Aktürk, M. Uneeb, R. Gohar, The effect of number of balls and preload on vibrations associated with ball bearings. ASME Journal of Tribology; 119 (1997), 747–753.
[7] N. Aktürk. The Effect of Waviness on Vibrations Associated With Ball Bearings, ASME Journal of Tribology, 121 (1999), 667-677.
[8] S.P. Harsha, K. Sandeep,R. Prakash . Nonlinear dynamic behaviors of rolling element bearings due to surface waviness. Journal of Sound and Vibration, 272 (2004), 557–580.
[9] S.P. Harsha, P.K. Kankar. Stability analysis of a rotor bearing system due to surface waviness and number of balls. International Journal of Mechanical Sciences 46(2004), 1057-1081.
[10] S.P. Harsha, C. Natraj and P.K. Kankar. The effect of ball waviness on nonlinear vibration associated with rolling element bearing. International Journal of Acoustics and Vibration 11(2006), 56-66.
[11] T. A. Harris. Rolling Bearing Analysis, Wiley, New York, 2001.

Appendix A: Contact Deformation

For pure point/line contact, the potential energy related with the contact is calculated form the theory of Hertzian contact deformation (Harris, [11]), the relationships for a point contact in ball bearings is a force expression with the displacement raised to an exponent (p) of $3/2$.

Where $k_{in}\int_0^{\delta_{in}}\left(\left(k_{in\_contact}\right)\delta_{in}^{p}\right)d_f$ (A.1)

$$k_{in}=\frac{1}{p+1}k_{in\_contact}\delta_{in+}^{p+1} \tag{A.2}$$

Now the generalized part of potential energy is $\frac{1}{p+1}k_{in}\delta_{in+}^{2}$

$$\frac{1}{p+1}k_{in\_contact}\delta_{in+}^{p+1}=\frac{1}{p+1}k_{in}\delta_{in+}^{2} \tag{A.3}$$

Hence, for ball bearing (p=3/2) stiffness at inner and outer race is,

$$k_{in}=k_{in\_contact}\sqrt{\delta_{in+}} \tag{A.4}$$

$$k_{out} = k_{out\_contact} \sqrt{\delta_{out+}} \tag{A.5}$$

With the consideration of surface waviness (Π_{in}), the contact deformations at the inner and outer races are:

$$\delta_{in} = \left[\{r + \rho_r + +\Pi_{in}\} - \chi_j\right] \tag{A.6}$$

$$\delta_{out} = \left[R - \{\rho_j + \rho_r + +\Pi_{in}\}\right] \tag{A.7}$$

Appendix B: Contact Damping

For the j[th] rolling element the equivalent contact stiffness between the rolling element and race is

$$k_{Eq} = \tfrac{3}{2} k_{contact} \quad \delta^{1/2} \tag{B.1}$$

The deforming forces for the j^{th} rolling element and inner race is [Harris, [11]]

$$F_{d\_in} = C_{in}\ k_{Eq} \left(\dot{\delta}_{in}\right)_+^p \tag{B.2}$$

$$F_{d\_in} = \frac{3}{2} C_{in} \left(k_{in\_contact}\right) \delta_{in+}^{1/2}\ \dot{\delta}_{in+}^{p} \tag{B.3}$$

Similarly, the damping force for the j^{th} the rolling element with the outer race is:

$$F_{d\_out} = C_{out} \delta_{out+} k_{eq} \tag{B.4}$$

$$F_{d\_out} = \frac{3}{2} C_{out} \left(k_{out\_contact}\right) \delta_{out+}^{1/2}\ \dot{\delta}_{out+}^{p} \tag{B.5}$$

Hence total energy dissipation at both contact points of rolling element with inner and outer race is

$$E_{dissipation} = \frac{3}{2(p+1)} \sum_{j=1}^{N_{r.e.}} \left[\left\{ C_{in} \left(k_{in\_contact}\right) \delta_{in_+}^{3/2}\ \dot{\delta}_{in\ +}^{p+1} \right\} + \left\{ C_{out} \left(k_{out\_contact}\right) \delta_{out_+}^{3/2}\ \dot{\delta}_{out+}^{p+1} \right\} \right] \tag{B.6}$$

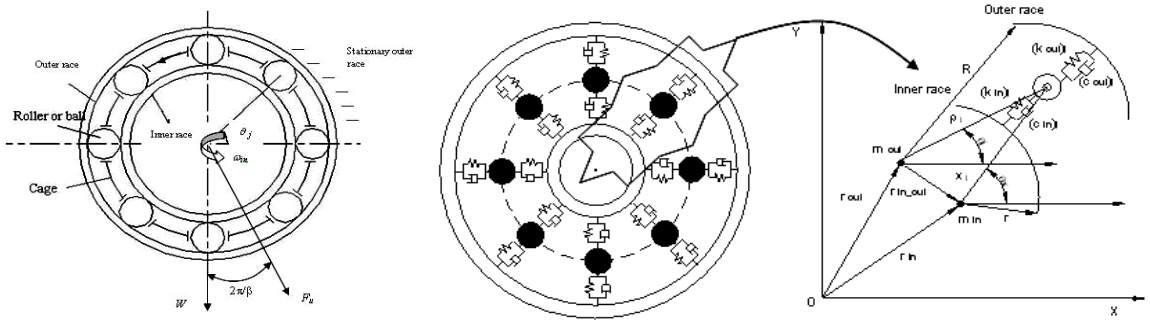

Fig. 1 a) Schematic diagram of rolling element bearings **(b)** Mass – spring - damper model

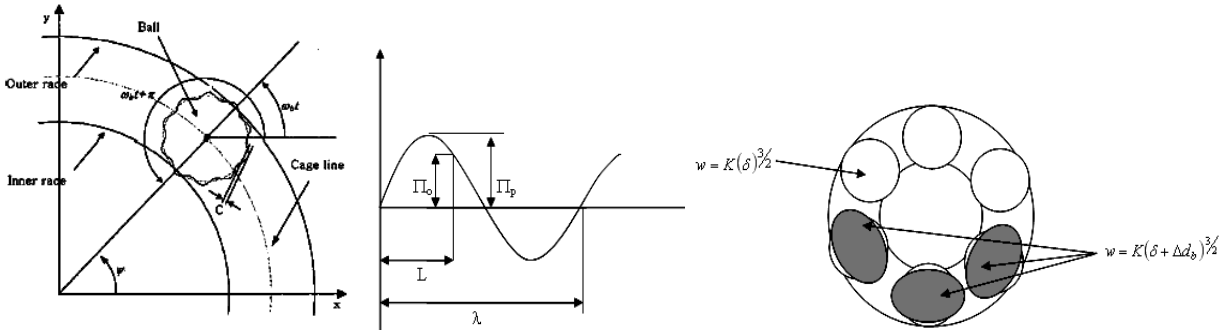

Fig. 2(a) Wavy feature of rolling elements **(b)** Wave of the Race **(c)** off-sized balls in a set of balls

Rolling Elements Defects: Case – I: Off-sized Rolling Elements

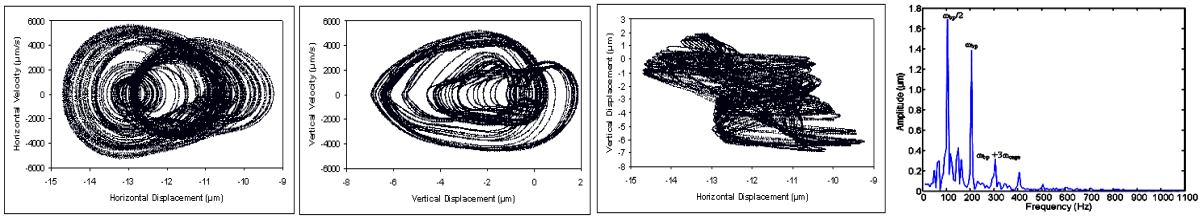

(a)

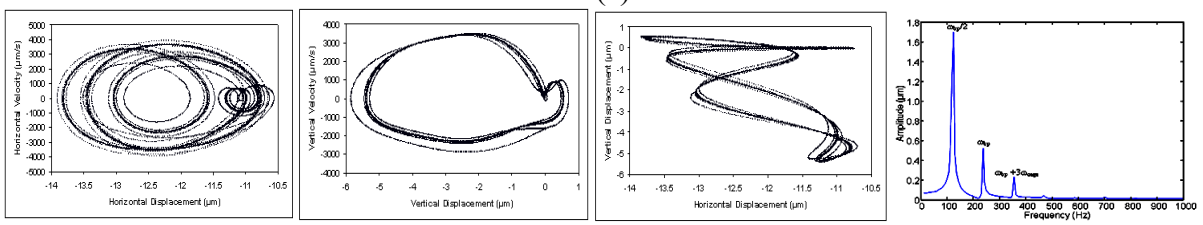

(b)

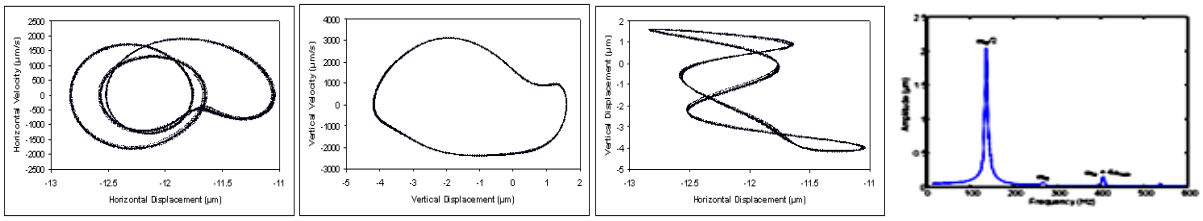

(c)

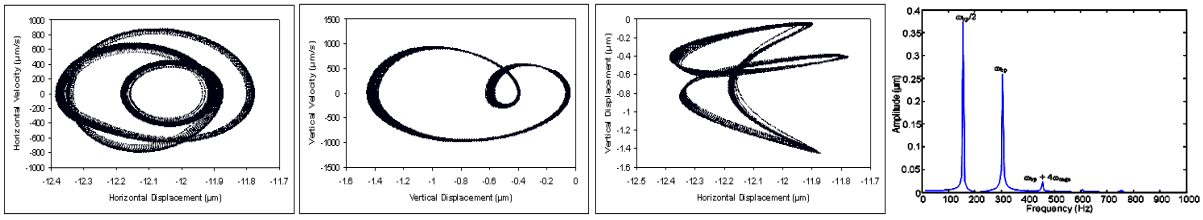

(d)

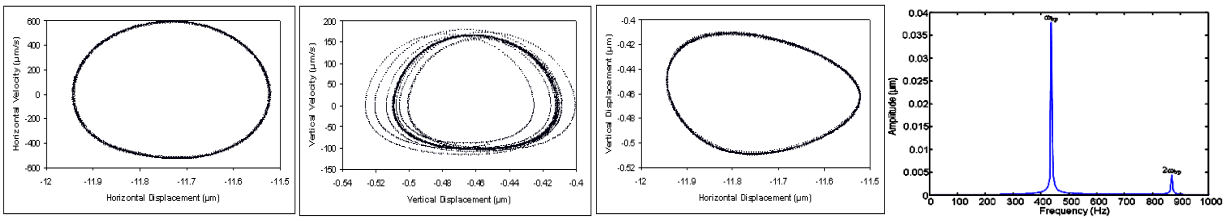

(e)

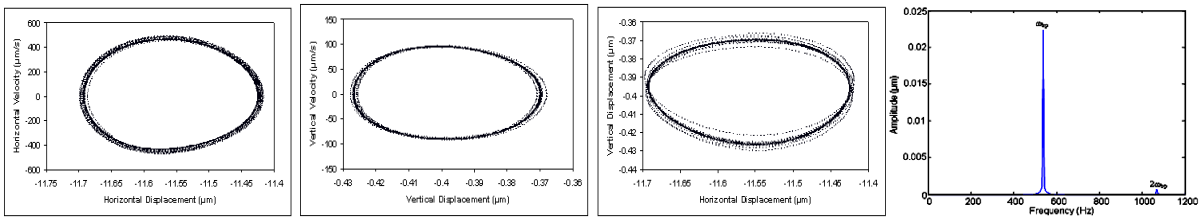

(f)

Fig. 3 Poincaré Maps, Orbit Plots and FFT for varying off-sized rolling elements (a) N_b = 6, (b) N_b = 7 (c) N_b = 8 (d) N_b = 9 (e) N_b = 13 (f) N_b = 16

Case – II: Rolling Elements Waviness

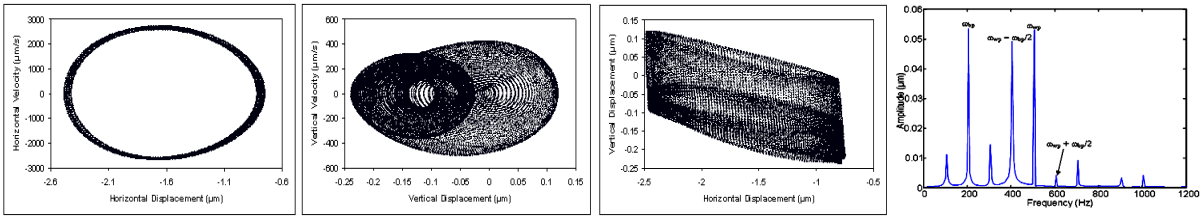

(a)

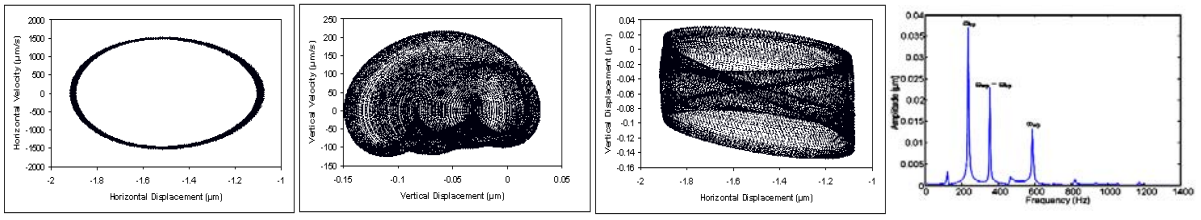

(b)

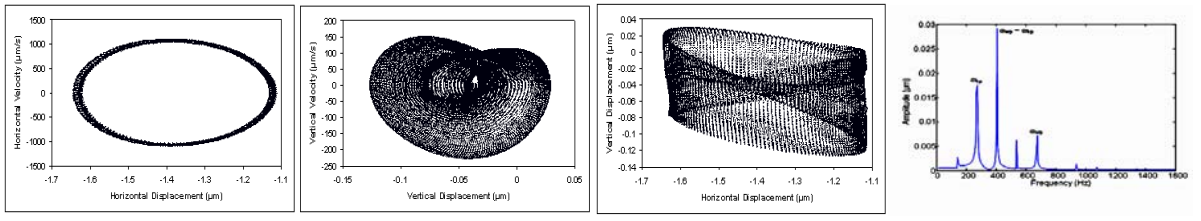

(c)

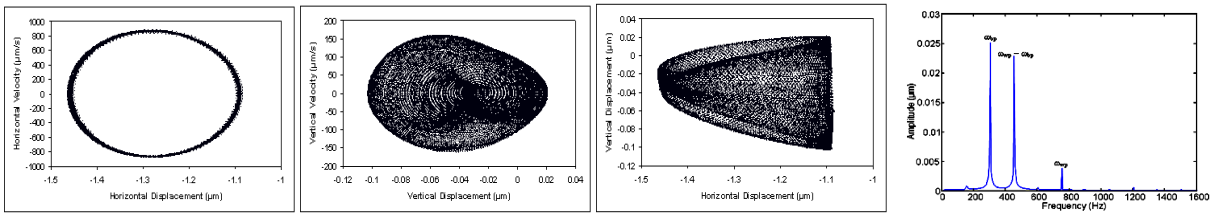

(d)

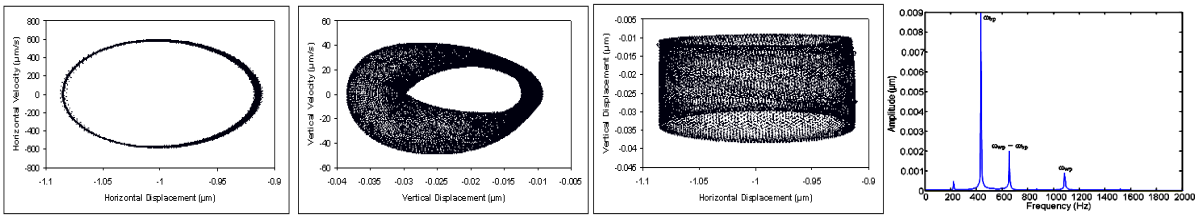

(e)

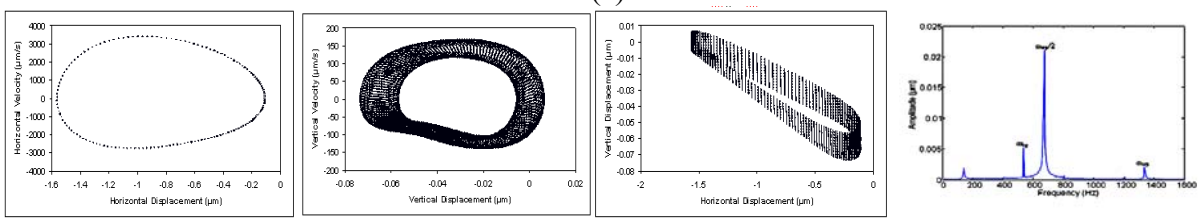

(f)

Fig. 4 Poincaré Maps, Orbit Plots and FFT for Wavy rolling elements (a) N_b=6 & N_w=6 (b) N_b=7 & N_w=7 (c) N_b=8 & N_w=8 (d) N_b=9& N_w=9 (e) N_b=13& N_w=13 (f) N_b=16& N_w=16

Received: October, 2008